Macromolecular Design Strategies for Preventing Active-Material Crossover in Non-Aqueous All-Organic Redox-Flow Batteries

Sean E. Doris,[a] Ashleigh L. Ward,[b] Artem Baskin,[b] Peter D. Frischmann,[b] Nagarjuna Gavvalapalli,[c] Etienne Chénard,[c] Christo S. Sevov,[d] Melanie S. Sanford,[d] David Prendergast,[b][e] Jeffrey S. Moore,[c] and Brett A. Helms*[b][e]

Abstract: Intermittent energy sources, including solar and wind, require scalable, low-cost, multi-hour energy storage solutions in order to be effectively incorporated into the grid. All-organic non-aqueous redox-flow batteries offer a solution, but suffer from rapid capacity fade and low Coulombic efficiency due to the high permeability of redox-active species across the battery's membrane. Here we show that active-species crossover can be arrested by scaling the membrane's pore size to molecular dimensions and in turn increasing the size of the active material to be above the membrane's pore-size exclusion limit. When oligomeric redox-active organic molecules (ROMs) were paired with microporous polymer membranes, the rate of active-material crossover was slowed more than 9,000-fold compared to traditional separators at minimal cost to ionic conductivity. This corresponds to an absolute rate of ROM crossover of less than 3 µmol cm^{-2} day^{-1} (for a 1.0 M concentration gradient), which exceeds performance targets recently set forth by the battery industry. This strategy was generalizable to both high and low-potential ROMs in a variety of non-aqueous electrolytes, highlighting the importance of macromolecular design in implementing next-generation redox-flow batteries.

All-Organic redox-flow batteries are well positioned to offer low-cost, multi-hour electrochemical energy storage at large scale in line with targets for grid modernization.[1-5] During flow-battery operation, solutions of redox-active organic molecules (ROMs) in a non-aqueous electrolyte are circulated through the negative and positive electrode compartments of an electrochemical cell. These compartments are electronically isolated from each other by a separator or ion-conducting membrane.[6,7] In order to maximize cycle-life and efficiency, it is imperative to block ROMs from migrating between electrode compartments during cycling while also maintaining facile transport of the working ion.[8]

Here we show how this can be achieved through the development of new macromolecular design principles advanced and applied to ROMs and ion-selective membranes derived from polymers of intrinsic microporosity (PIMs). In contrast with traditional mesoporous battery separators, membranes derived from PIMs feature permanent micropores that in principle could allow working-ion conduction while blocking the crossover of larger active-materials.[9-13] Indeed, we found that the effective diffusion coefficient (D_{eff}) for small-molecule ROMs (e.g., **1a**) through PIM-1 membranes decreased 40-fold compared to a Celgard separator with ~20 nm pores. Additional gains in blocking ability (470-fold) were obtained with chemically cross-linked PIM-1 membranes, which restrict pore swelling in electrolyte. While these gains alone are impressive, we hypothesized that increasing the effective size of the ROM, e.g., through oligomerization, would in turn provide active-materials that were larger than the PIM membrane's pore-size exclusion limit and thereby enable active-material blocking through a size-sieving mechanism. Indeed, by increasing slightly the molecular dimensions from 8.8 to 12.3 Å through oligomerization, D_{eff} fell below our experimental limit of quantification, with an estimated upper-bound of 3.4×10^{-11} cm^2 s^{-1} (Fig. 2). Despite this dramatic 9,000-fold improvement in membrane blocking ability relative to Celgard, PIM-1 membranes retained high ionic conductivities of at least 0.4 mS cm^{-1} (compared to 2.2 mS cm^{-1} for Celgard). Furthermore, we found that sieving oligomeric organic active materials by size with PIM membranes was preserved for different ROM chemistries (e.g., **3b** and **3c**) in a variety of battery electrolytes (e.g., ACN, PC, DME, etc), highlighting the generality of our approach.

Breaking with convention, the advances reported here provide an important counterpoint to: 1) single-component electrodes paired with ceramic membranes, which are expensive and difficult to scale;[14] 2) thick macroporous separators paired with mixed-electrode formulations (i.e., anolytes and catholytes present in both electrode compartments), which lead to Coulombic inefficiencies and short cycle-life;[15,16] and 3) mesoporous separators paired with redox-active polymers, which can be difficult to pump through electrochemical cells at high molecular weight and at all states-of-charge.[17,18] Our strategy to implement ROM oligomerization, as opposed to polymerization, should also serve to retain the facile charge transfer kinetics that are characteristic of ROM monomers, which is essential for power quality and high active-material utilization.[19]

[a] S.E. Doris
Department of Chemistry
419 Latimer Hall, University of California, Berkeley
Berkeley, CA 94720, USA

[b] Dr. A.L. Ward, Dr. P.D. Frischmann, Dr. A. Baskin, Dr. D. Prendergast, Dr. B.A. Helms*
Joint Center for Energy Storage Research
Lawrence Berkeley National Laboratory
1 Cyclotron Road, Berkeley, CA 94720, USA
E-mail: bahelms@lbl.gov

[c] Dr. N. Gavvalapalli, Dr. E. Chénard, Prof. J.S. Moore
Joint Center for Energy Storage Research
University of Illinois at Urbana-Champaign
505 South Matthews Avenue
Urbana, IL 61801, USA

[d] Dr. C. S. Sevov, Prof. M. S. Sanford
Joint Center for Energy Storage Research
University of Michigan
930 North University Avenue
Ann Arbor, MI 48109, USA

[e] Dr. D. Prendergast, Dr. B.A. Helms*
The Molecular Foundry
Lawrence Berkeley National Laboratory
1 Cyclotron Road, Berkeley, CA 94720, USA

Supporting information for this article is given via a link at the end of the document.
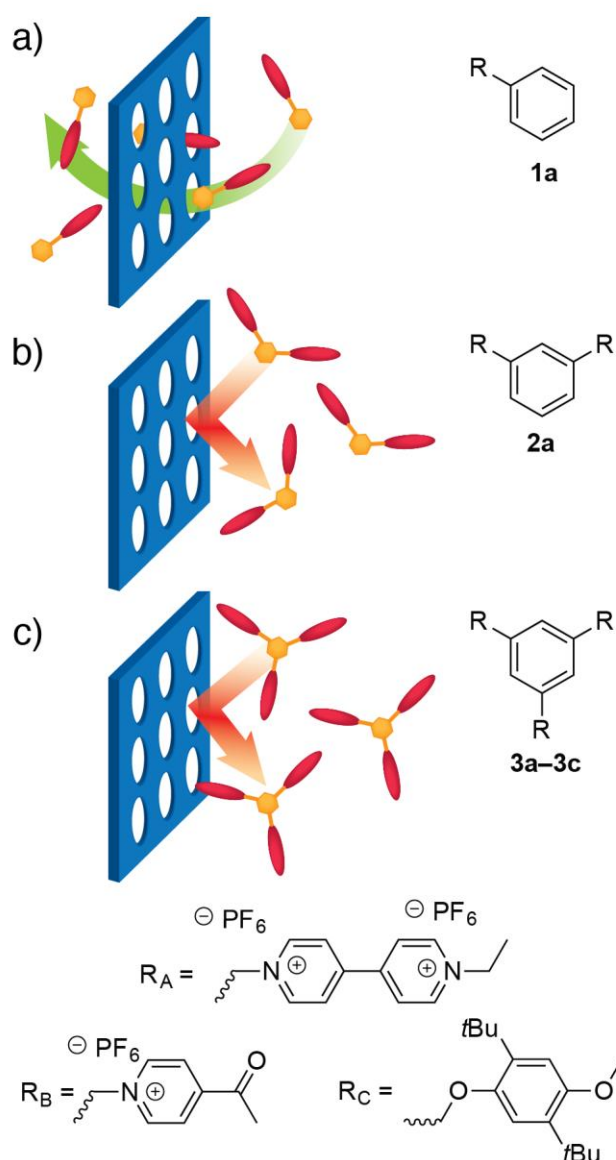
Figure 1. Macromolecular design strategies for preventing active-material crossover in all-organic redox-flow batteries: a) Small-molecule redox-active organic molecules (ROMs) pass through microporous membranes; b) and c) larger redox-active oligomers (RAOs) are blocked from passing through the membrane by a size-sieving mechanism.

To quantitatively inform the critical size regime for ROM-blocking by a size-selective polymer membrane, we designed a series of viologen-based redox-active oligomers (RAOs) (**1a**–**3a**, Fig. 1) and studied their solvated structures computationally in acetonitrile (ACN) using a combination of ab initio quantum mechanical studies and classical molecular dynamics simulations (see SI, Figs. S1–S5, Tables S1–2). Our RAO design was structurally minimal, with redox-active viologens serving as pendants to a central mesitylene core (Fig. 1). We were interested in understanding active-material solvation at different states of charge (SOCs), as changes in solvation may affect the crossover behavior as the battery is cycled. We found

that ACN molecules are preferentially oriented at solvent-viologen interfaces, with electron-rich nitriles stabilizing the cationic viologen pendants at all SOCs (see new Fig. SS5). For each redox-active oligomer, we calculated the average number of ACN molecules as a function of distance from the molecule's Van der Waals surface (Fig. 2) and found that the ROM solvation shells do not change significantly at different SOCs. This implies that membranes that are blocking to active-materials at one SOC will also block their crossover as the battery is cycled and the SOC changes. Furthermore, ACN molecules (and even PF_6^- counterions) in the solvation shell are only weakly associated with the ROMs, and the solvation of ROMs in ACN does not lead to significant changes in their structural conformation with respect to isolated geometries. Therefore, the hydrodynamic radii and associated volumes of ROMs can be computed from quantum mechanical calculations of isolated clusters. Characteristic sizes for viologen monomer (**1a**), dimer (**2a**) and trimer (**3a**) were 8.8, 12.3, and 16.8 Å, respectively. These results suggest that polymer membranes whose pore dimensions were maintained below 1.2 nm would be effective in blocking the viologen dimer and trimer; considerably smaller pores would be required to sieve the monomer.

To validate the theoretical predictions of a critical size-regime for ROM-blocking, we synthesized the viologen-based ROM monomer (**1a,** 84%), dimer (**2a,** 80%), and trimer (**3a,** 69%) by a simple displacement reaction involving *N*-ethyl-4,4'-bipyridinium hexafluorophosphate and benzyl bromide, 1,3-bis(bromomethyl)benzene, and 1,3,5-tris(bromomethyl)benzene, respectively. Cyclic voltammetry of each compound showed that **1a**, **2a**, and **3a** are reversibly reduced at –0.75 V *vs.* Ag/Ag$^+$ (Fig. S6, Table S3). This low reduction potential along with the high solubility of each species in ACN is promising for their use as energy dense anolytes in all-organic redox flow batteries.[1] The crossover behavior for each ROM/membrane pairing was quantified by measuring the effective diffusion coefficient (D_{eff}) of each ROM through different membranes (Fig. 3, Figs. S7–8, see SI for details). By comparing the ROM's diffusion coefficient through the membrane (D_{eff}) to its diffusion coefficient through solution (D_{sol}), the membrane's blocking ability can be quantified. For the non-selective Celgard membrane, high values for D_{eff} of $(5.4 \pm 0.4) \times 10^{-7}$, $(3.1 \pm 0.3) \times 10^{-7}$, and $(2.2 \pm 0.2) \times 10^{-7}$ cm^2 s^{-1} for **1a**, **2a**, and **3a**, respectively, were measured. These measured values of D_{eff} are only 30-fold lower than D_{sol} for each ROM, indicating that the blocking-ability of Celgard is poor, and that it blocks **1a**, **2a**, and **3a** equally poorly. PIM-1 membranes, which feature nanometer-sized pores, significantly outperformed Celgard, with **1a**, **2a**, and **3a** diffusing through the membrane 1,280, 11,600, and 32,900-fold slower, respectively, than through solution (Fig. 3b). This dramatic improvement in membrane blocking-ability upon reducing the pore size from approximately 20 nm to less than 1 nm, along with the improved membrane blocking-ability for larger ROMs, is indicative of size-selective blocking of active-materials. However, our theoretical calculations of the sizes of **2a** and **3a** imply that they should be completely blocked by PIM-1 membranes. We hypothesized that this discrepancy was a result of the PIM-1 membranes swelling
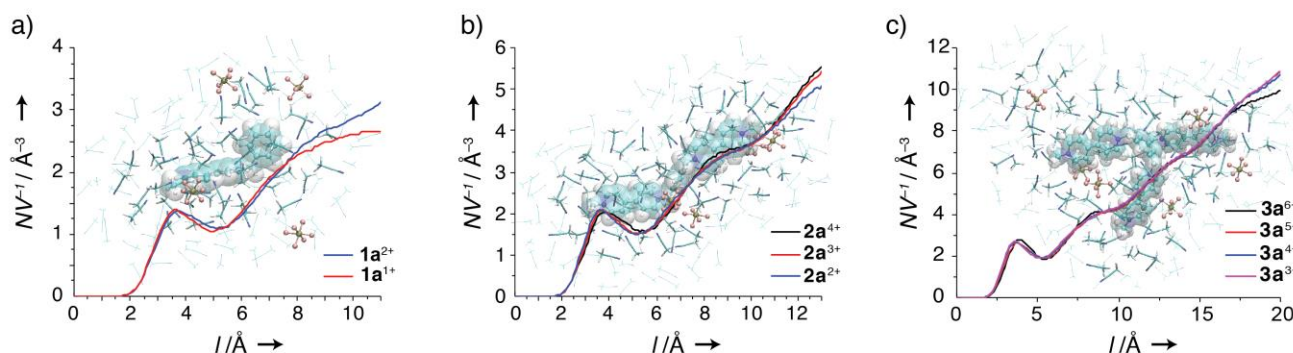
Figure 2. Solvated structures of a) **1a**, b) **2a**, and c) **3a** for different states-of-charge. The density of ACN molecules (NV^{-1}) as a function of distance (l) from each molecule's Van der Waals surface does not vary dramatically at different states of charge; solvated molecular conformations are similar to isolated analogs, and characteristic sizes of 8.8, 12.3, and 16.8 Å were calculated from quantum mechanical calculations of isolated clusters.

significantly in electrolyte, thus increasing the average pore size above the 0.9 nm pores present in dry membranes.[20]

By cross-linking PIM-1, the degree of swelling can be controlled, and the membrane pore size can be further constricted. This was accomplished by casting solutions of PIM-1 containing the cross-linking agent 2,6-bis(4-azidobenzylidene)-cyclohexanone. The dry membranes were then heated to 175 °C under vacuum to convert the azide groups of the cross-linking agent to reactive nitrenes, which inserts into C-H bonds on the polymer and cross-links the membranes (Fig. S9).[10,21] Cross-linked PIM-1 membranes exhibited the best active-species blocking-ability observed to date, with **1a** diffusing through the membrane 14,200-fold slower than through solution, and **2a** and **3a** diffusing slower than the limit of quantification (297,000 and 85,000-fold slower, respectively, than through solution). This unprecedented 9,000-fold improvement in blocking ability (with respect to Celgard) came at minimal cost to ionic conductivity, with cross-linked PIM-1 membranes only 5-fold less conductive than Celgard (0.4 *vs.* 2.2 mS cm^{-1}, see Fig. S10–11).

To demonstrate that oligomerization is a generalizable approach to blocking ROM crossover in all-organic non-aqueous redox flow batteries, we synthesized trimeric RAOs based on acylpyridinium hexafluorophosphates (**3b**, 89%) and DB3 (**3c**, 90%) redox-active pendant groups. Monomeric forms of these ROMs have been identified as promising candidates for non-aqueous redox-flow batteries, although their crossover through the battery membrane remains an issue that needs to be solved.[2,3] Consistent with these reports, cyclic voltammetry showed evidence for reversible reduction of **3b** at –1.40 V *vs.* Ag/Ag$^+$ in 0.1 M TBAPF$_6$/propylene carbonate. Likewise, **3c** underwent reversible oxidation at 0.56 V *vs.* Ag/Ag$^+$ in 0.1 M TBAPF$_6$/dimethoxyethane. Both **3b** and **3c** were blocked by cross-linked PIM-1 membranes, with **3b** diffusing through the membrane slower than the lower limit of quantification of 3.8 × 10^{-11} cm^2 s^{-1} and **3c** diffusing through the membrane with D_{eff} = (8.1 ± 0.7) × 10^{-10} cm^2 s^{-1} (Fig. 4). This corresponds to 6,800 and 460-fold improvements in the crossover rate of **3b** and **3c**, respectively, when compared to their diffusion through non-selective mesoporous separators. Clearly, oligomerization provides a straightforward path to preparing a wide variety of
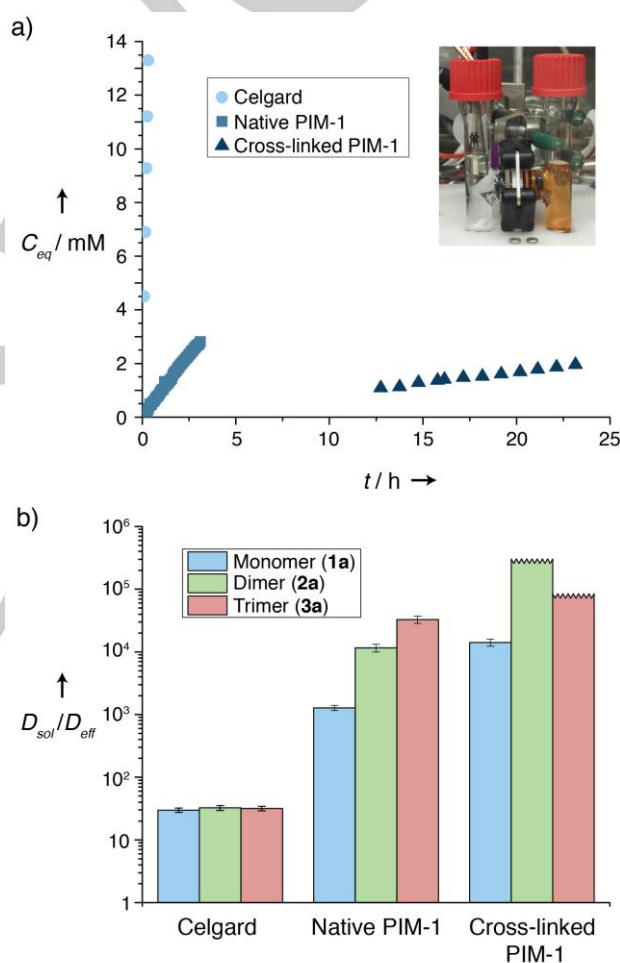

Figure 3. a) Concentration (C_{eq}) of **1a** in the permeate compartment as a function of time (t) (adjusted for membrane thickness to allow comparisons between different membranes) for Celgard, native PIM-1, and cross-linked PIM-1 membranes (inset) picture of the crossover cell used to measure D_{eff}, b) Membrane blocking ability for each membrane paired with ROMs **1a**–**3a**. D_{sol}/D_{eff} is a figure-of-merit that describes how much slower the molecule diffuses through the membrane than through solution. The diffusion of **2a** and **3a** through the cross-linked PIM-1 membranes was slower than the lower limit of quantification, so the maximum possible value is indicated by jagged lines.
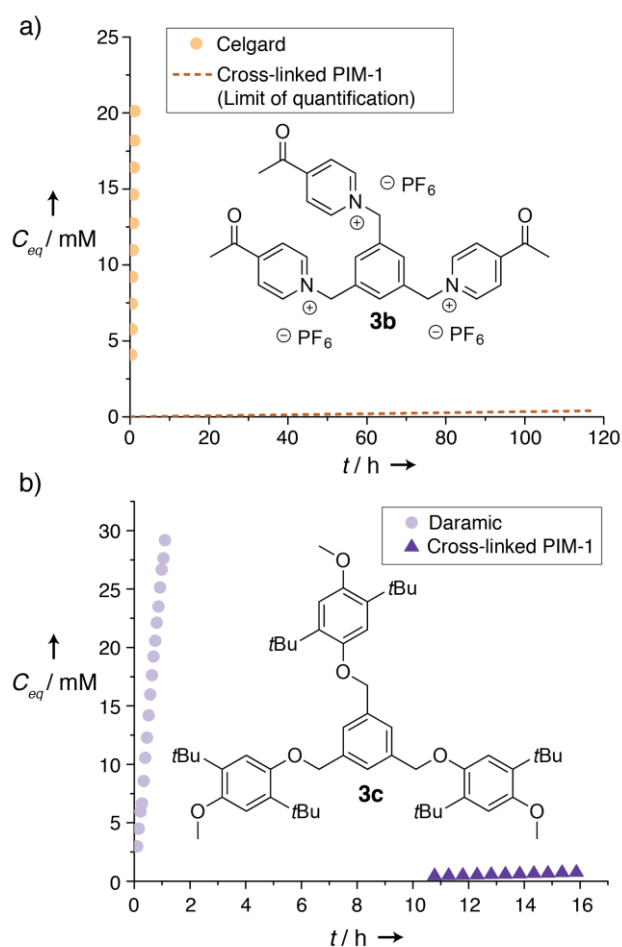
a)

b)

Figure 4. ROM concentration (C_{eq}) in the permeate compartment as a function of time (t) for a) **3b** and b) **3c** paired with non-selective mesoporous and cross-linked PIM-1 membranes. The dashed line in a) indicates the steepest possible slope for **3b** diffusing through cross-linked PIM-1, as this experiment never reached the lower limit of quantification and is an indicator that a true size-sieving mechanism is at play.

ROMs that can be effectively blocked by microporous polymer membranes.

Macromolecular design of both membranes and active-species is a powerful approach for solving the crossover problem in all-organic redox-flow batteries. Here we showed how computational chemistry informs the design space for ROM oligomers, or RAOs, and that by pairing RAOs with RAO-blocking microporous PIM membranes, active material crossover can be reduced by nearly four orders of magnitude with respect to commercially available battery separators with negligible decreases in ionic conductivity. ROM oligomerization was demonstrated for several redox-active motifs, including those that serve as either negative and positive electrode materials in redox-flow batteries. In all cases, RAO crossover was effectively blocked when constituted as flowable electrodes in a variety of battery solvents, including acetonitrile, propylene carbonate, and 1,2-dimethoxyethane. These promising results point the way forward towards the design of new classes of ROMs and membranes for all-organic redox-flow batteries,

along with their incorporation in next-generation redox-flow battery prototypes.

Experimental Section

Materials and methods, synthetic details, characterization, and membrane preparation are all described in the Supporting Information. All membranes were soaked in electrolyte (0.1 M LiPF$_6$ in ACN for **1a–3a**, 0.1 M TBAPF$_6$ in PC for **3b**, or 0.1 M TBAPF$_6$ in DME for **3c**) for at least 12 h before use. Equivalent concentration (C_{eq}) refers to the concentration of ROM that would be observed with a 10 μm membrane and $C_0 = 0.1$ M. This allows for easier visual comparison of crossover experiments performed with different membrane thicknesses (raw data can be found in the Supporting Information).

[1]   R. M. Darling, K. G. Gallagher, J. A. Kowalski, S. Ha, F. R. Brushett, *Energy Environ. Sci.* **2014,** *7*, 3459.

[2]   F. R. Brushett, J. T. Vaughey, A. N. Jansen, *Adv. Energy Mater.* **2012,** *2*, 1390.

[3]   C. S. Sevov, R. E. M. Brooner, E. Chénard, R. S. Assary, J. S. Moore, J. Rodríguez-López, M. S. Sanford, *J. Am. Chem. Soc.* **2015,** *137*, 14465.

[4]   B. Dunn, H. Kamath, J.-M. Tarascon, *Science* **2011,** *334*, 928.

[5]   W. Wang, Q. Luo, B. Li, X. Wei, L. Li, Z. Yang, *Adv. Funct. Mater.* **2013,** *23*, 970.

[6]   P. Arora, Z. Zhang, *Chem. Rev.* **2004,** *104*, 4419.

[7]   S.-H. Shin, S.-H. Yun, S.-H. Moon, *RSC Adv.* **2013,** *3*, 9095.

[8]   R. M. Darling, K. G. Gallagher, W. Xie, L. Su, F. R. Brushett, *J. Electrochem. Soc.* **2016,** *163*, A5029.

[9]   C. Li, A. L. Ward, S. E. Doris, T. A. Pascal, D. Prendergast, B. A. Helms, *Nano Lett.* **2015,** *15*, 5724--5729.

[10]   S. E. Doris, A. L. Ward, P. D. Frischmann, L. Li, B. A. Helms, *J. Mater. Chem. A* **2016,** *In press*, DOI: 10.1039/c6ta06401a.

[11]   N. B. McKeown, P. M. Budd, *Chem. Soc. Rev.* **2006,** *35*, 675.

[12]   P. M. Budd, B. S. Ghanem, S. Makhseed, N. B. McKeown, K. J. Msayib, C. E. Tattershall, *Chem. Commun.* **2004,** , 230.

[13]   N. B. McKeown, P. M. Budd, *Macromolecules* **2010,** *43*, 5163.

[14]   P. Knauth, *Solid State Ionics* **2009,** *180*, 911--916.

[15]   W. Duan, R. S. Vemuri, J. D. Milshtein, S. Laramie, R. D. Dmello, J. Huang, L. Zhang, D. Hu, M. Vijayakumar, W. Wang, J. Liu, R. M. Darling, L. Thompson, K. Smith, J. S. Moore, F. R. Brushett, X. Wei, *J. Mater. Chem. A* **2016,** *4*, 5448.

[16]   X. Wei, W. Xu, J. Huang, L. Zhang, E. Walter, C. Lawrence, M. Vijayakumar, W. A. Henderson, T. Liu, L. Cosimbescu, B. Li, V. Sprenkle, W. Wang, *Angew. Chem., Int. Ed.* **2015,** *54*, 8684.

[17]   G. Nagarjuna, J. Hui, K. J. Cheng, T. Lichtenstein, M. Shen, J. S. Moore, J. Rodríguez-López, *J. Am. Chem. Soc.* **2014,** *136*, 16309.

[18]   M. Burgess, J. S. Moore, J. Rodríguez-López, *Acc. Chem. Res.* **2013,** *Article ASAP*, 10.1021/acs.accounts.6b00341.

[19]   M. Burgess, E. Chénard, K. Hernandez-Burgos, G. Nagarjuna, R. S. Assary, J. Hui, J. S. Moore, J. Rodríguez-López, *Chem. Mater.* **In press,** , .

[20]   C. L. Staiger, S. J. Pas, A. J. Hill, C. J. Cornelius, *Chem. Mater.* **2008,** *20*, 2606.

[21]   N. Du, M. M. Dal-Cin, I. Pinnau, A. Nicalek, G. P. Robertson, M. D. Guiver, *Macromol. Rapid Commun.* **2011,** *32*, 631.

Entry for the Table of Contents

COMMUNICATION

Better Sieving Through Chemistry: Macromolecular chemistry provides a general approach for blocking redox-active organic molecules (ROMs) from crossing through battery membranes at minimal cost to ionic conductivity. This advance solves a critical challenge facing next-generation redox-flow batteries, clearing the way toward efficient, low-cost grid-scale energy storage.

((Insert TOC Graphic here))

S.E. Doris, A.L. Ward, A. Baskin, P.D. Frischmann, N. Gavvalapalli, E. Chénard, C.S. Sevov, M.S. Sanford, D. Prendergast, J.S. Moore, B.A. Helms*

Page No. – Page No.

Macromolecular Design Strategies for Preventing Active-Material Crossover in Non-Aqueous All-Organic Redox Flow Batteries